J Mater Sci (2007) 42:4051–4059
DOI 10.1007/s10853-006-0187-4

Superplastic power-law creep of Sn–40%Pb–2.5%Sb peritectic alloy

R. Mahmudi · A. Rezaee-Bazzaz

Received: 10 May 2005 / Accepted: 10 April 2006 / Published online: 31 January 2007

Abstract The power law-creep behavior of superplastic Sn–40Pb–2.5Sb alloys with different grain sizes has been investigated at room temperature. Stress exponent values for these alloys have been determined by indentation creep, conventional creep and uniaxial tension tests in order to evaluate the correspondence of indentation creep results with conventional tests. In all cases, the indentation results were in good agreement with each other and with those of the tensile and conventional creep tests. The average stress exponent values of about 2.6 and 3.0 corresponding to the strain rate sensitivity (SRS) indices of 0.33–0.39, depending on the grain size of the materials, indicate that the grain boundary sliding is the possible mechanism during creep deformation of Sn–Pb–Sb alloys. Within limits, the indentation tests are thus considered useful to acquire information on the creep behavior of small specimens of these soft tin–lead–antimony alloys at room temperature. It is also demonstrated that the indentation creep test provides a convenient method to measure SRS and thereby to assess the ability of a material to undergo superplastic deformation.

Introduction

Tin–lead alloys are the most widely used solders which are used for joining most materials used in the electronic industries. Antimony may be added to Sn–Pb alloys as a substitute for some of the tin. This effectively reduces the cost per unit of the solder [1] and improves the strength properties of the material [2]. It has been reported that solid solution strengthening of Sn occurs with up to 7% Sb, and since the solubility of Sn in Pb at room temperature is small, the solid solution strengthening of Sn–Pb solder by antimony is due mainly to strengthening of the tin [3]. To date, most of the experimental results for room temperature superplasticity and creep of lead alloys relate to the Pb–Sn eutectic [4–6]. This alloy has extensively been used as a model material because it can maintain a small and reasonably stable grain size at room temperature. By introducing 2.5% Sb in the Sn–Pb eutectic alloy, a Sn–40%Pb–2.5%Sb peritectic is developed which possesses good mechanical properties and lower cost. The contact angle for this alloy is higher (28°± 3°) than that of lead–tin eutectic (17°± 4°), but is considered adequate from wettability considerations [7]. Knowing that the peritectic temperature of this alloy is 462 K, ambient operating temperature and local heating during operation correspond to homologous temperatures greater than 0.65 for this solder alloy [8]. Therefore, creep behavior of the material is of great interest mainly due to the need for attaining shape and mechanical properties.

Several papers have addressed the possibility of gaining information on creep properties by the use of indentation or long time hardness tests [4, 9–11]. Indentation creep is a well-known test technique, which has been applied in the study of non-metallic solids [12], pure metals [13], polycrystalline materials [14–16] and composites [17]. When a constant load is applied on the surface of a sample with a suitable

R. Mahmudi (✉) · A. Rezaee-Bazzaz
Department of Metallurgical and Materials Engineering, Faculty of Engineering, University of Tehran, P.O. Box 11365-4563, Tehran, Iran
e-mail: mahmudi@ut.ac.ir

indenter over a period of time, plastic yield and creep take place as the indenter penetrates the material. The variation in the indentation size, expressed either as a change in diameter (Brinell test), diagonal length (Vickers test), or penetration depth of a cylindrical indenter (Impression test) is monitored with dwell time. Thus, the time-dependent flow behavior of materials can be studied by these simple hardness tests. This can be particularly advantageous when the material is only available as small test-pieces or there are some difficulties with the machining of samples made of very soft materials. Therefore, the indentation creep tests, regarded as a quick, simple and non-destructive procedure to extract information on the mechanical behavior of materials, greatly reduce the effort for sample preparation [18, 19].

The superplasticity of Pb–62.8%Sn eutectic alloy has been studied using indentation creep by some researchers [5, 6]. These investigations have shown that superplastic deformation of this alloy occurs in the temperature range of 283–340 K with the creep activation energy being in the range of 45.8–58.1 kJ/mol, which is in good agreement with those obtained in conventional creep tests. Superplasticity of Zn–22%Al eutectoid alloy has also been investigated using this technique by Yu et al. [20] and Kumar et al. [21]. Results of these works showed that indentation creep test can be used to investigate superplastic deformation, where the parameters which are commonly considered as characteristics of superplasticity can be obtained. In addition to superplastic materials, indentation creep has also been used for studying creep properties of other materials. Chinh et al. [22] used indentation creep for analyzing creep behavior of an AlMgZn alloy with special interest in calculating threshold stress. Cseh et al. [17] studied creep properties of a short fiber reinforced metal-matrix composite and found a good agreement between creep rate and stress values obtained from impression creep and tensile creep experiments in the overlapping range of these two methods. Obtaining the creep properties of a 316 stainless steel [23] and a TiAl alloy [24] has been also reported in the literature where, there has been a good agreement between indentation creep and conventional creep results. This technique has also been used for studying the creep properties of high temperature materials such as intermetallics and ceramics, including diamond, which are very difficult to evaluate using conventional methods [19].

As mentioned before, the majority of research works on the indentation creep behavior of solder alloys have been focused on the eutectic Pb–62.8%Sn alloy. However, other solder materials such as Pb–9%Sn [25] and more recently Sn–3.5%Ag [26, 27], have also been studied by indentation and impression testing techniques. On the other hand, the creep behavior of the Sn–Pb–Sb alloys has been rarely studied even by conventional creep tests and thus, a thorough investigation of their room-temperature creep behavior using tension, indentation and conventional creep tests would be attempted in this investigation.

Methods of indentation creep analysis

It is generally accepted that the mechanical behavior of metallic materials at homologous temperatures higher than 0.5 can be fairly expressed by the power-law creep in a wide range of strain rates [15, 28–30]. Thus, for steady-state creep, the relationship between the strain rate, $\dot{\varepsilon}$, and the tensile stress, σ, at a constant temperature can be expressed by:

$$\dot{\varepsilon} = A\sigma^n \tag{1}$$

where n is the steady-state stress exponent, defined as $n = \left[\frac{\partial \ln \dot{\varepsilon}}{\partial \ln \sigma}\right]_{\varepsilon}$, and A is a constant.

Mulhearn and Tabor [31] proposed an expression of the following form to acquire the steady-state stress exponent for pure lead at temperatures above $0.6T_m$:

$$-\left(n+\frac{1}{2}\right)\log H_V = \log t + B \tag{2}$$

where H_V is the Vickers number, t is the indentation dwell time and B is a constant. If hardness is plotted against time on a log–log scale, a straight line with slope $(n+\frac{1}{2})^{-1}$ is obtained.

Juhasz et al. [32] carried out tests on a superplastic lead–tin alloy using a Vickers indenter and obtained the stress exponent (n) in steady-state creep of the following form:

$$n = \left[\frac{\partial \ln \dot{d}}{\partial \ln H_V}\right]_d \tag{3}$$

where H_V is the Vickers hardness number, d is the indentation diagonal length and $\dot{d}$ is the rate of variation in indentation length. This implies that if $\dot{d}$ is plotted against H_V on a double logarithmic scale, a straight line would be obtained the slope of which is the stress exponent, n.

More recently, Sargent and Ashby [28] carried out hot hardness tests on a wide range of materials and proposed a dimensional analysis for indentation creep. According to their model, the displacement rate of an indenter has been derived as:

$$\frac{du}{dt} = \left[\frac{\dot{\varepsilon}_0}{C_2}\left(\sqrt{A}\right)\right]\left[\left(\frac{C_1}{\sigma_0}\right)\left(\frac{P}{A}\right)\right]^n \quad (4)$$

where A is the projected area of indentation, C_2 is a constant and $\dot{\varepsilon}_0$ is the rate at a reference stress σ_0, n is the stress exponent and P is the applied load. For a pyramid indenter the penetration is proportional to $\sqrt{A}$, i.e.,

$$u = C_3\sqrt{A} \quad (5)$$

Differentiating Eq. 5 with respect to time and substituting into Eq. 4 gives:

$$\frac{dA}{dt} = C_4\dot{\varepsilon}_0 A\left(\frac{P}{A}\sigma_0\right)^n \quad (6)$$

where C_3 and C_4 are constants. When P is held constant, Eq. 6 can be rewritten as:

$$\left(\frac{1}{H_V}\right)\left(\frac{dH_V}{dt}\right) = -C_4\dot{\varepsilon}_0\left(\frac{H_V}{\sigma_0}\right)^n \quad (7)$$

Sargent and Ashby have derived the following relationship between indentation hardness and dwell time:

$$H_V(t) = \frac{\sigma_0}{(nC_4\dot{\varepsilon}_0 t)^{\frac{1}{n}}} \quad (8)$$

where $H_V(t)$ is the time dependent hardness. Hence, from Eq. 8 the slope of a plot of $\ln(H_V)$ against $\ln(t)$ at a constant temperature is $-\frac{1}{n}$. Also from Eq. 7 a plot of $\ln\left[-\left(\frac{1}{H_V}\right)\left(\frac{dH_V}{dt}\right)\right]$ versus $\ln(H_V)$ at a constant temperature has a slope of n.

The aim of this paper is to investigate the superplastic power-law creep behavior of the peritectic Sn–40%Pb–2.5%Sb alloy at room temperature ($T > 0.5T_m$), by measuring the stress exponents and the corresponding SRS indices for the alloys having different grain sizes, using different methods of analysis for indentation creep. It is also intended to evaluate the applicability of indentation methods as compared with conventional creep and tensile tests.

Experimental procedure

Materials and processing

The material used was a peritectic Sn–40%Pb–2.5%–Sb alloy. It was prepared from high purity lead and tin (99.99%) and a Pb–20%Sb master alloy, melted in an electrical furnace under an inert argon atmosphere, and cast into $120 \times 30 \times 20$ mm slabs. In order to ensure that the slabs had similar initial microstructures, the slabs were homogenized at 403 K for 24 h. The slabs were rolled to 2.5 mm thick sheets at room temperature in order to generate a homogeneous fine-grained material without the initial as-cast dendritic structure. The sheets were then annealed at the temperatures of 370 and 430 K for 2 h. The specimens were examined by optical microscopy to observe the grain size and structure of the materials. These specimens were polished to a 0.25 microns diamond finish, followed by polishing on a microcloth without any abrasive. Etching was carried out using a 5% nitric acid and 95% alcohol solution. As shown in Fig. 1a, b, grain sizes of 2.4 and 5 μm were obtained for the materials annealed at 370 and 430 K, respectively.

Indentation creep tests

Square samples with edges of 20 mm were cut from the 2.5 mm thick rolled sheets. These samples were polished on a microcloth without using any abrasive and then tested in a Vickers hardness tester where the applied load and testing time were the only variables. In the Vickers test, a diamond pyramid with square

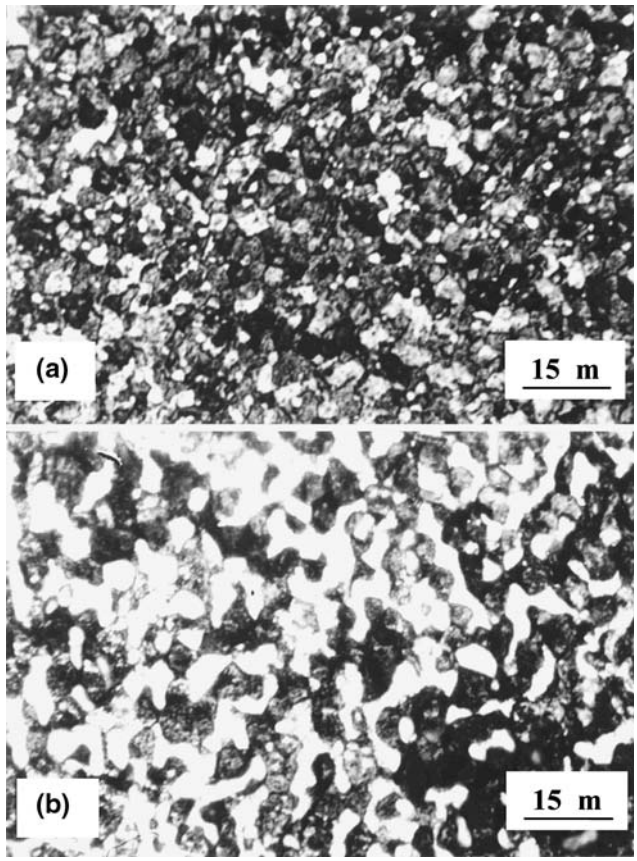

Fig. 1 Optical micrograph of the materials with (**a**) d = 2.4 μm; and (**b**) d = 5 μm

base was used where the Vickers hardness number was estimated from $H_V = 0.185F/d^2$, where F is the applied load in N and d is the average diagonal length in mm. Indentation hardness measurements were made on each sample using loads of 20, 30 and 50 N for dwell times up to 120 min. Each reading was an average of at least five separate measurements taken at random places on the surface of the specimens. All the indentations were at least 5 mm away from the edges and from other indentations. The maximum depth of penetration at 50 N load was about 0.2 mm.

Conventional creep tests

Specimens for creep tests were punched from the rolled sheets along the rolling direction. The specimens had gages 25 mm long and 6.5 mm wide. These were tested at room temperature under constant load in the range of 140–250 N, corresponding to initial stresses between 11 and 19 MPa. The specimen elongation was continuously recorded, using a digital dial gage connected to a computer data acquisition system, from which true strains were calculated and strain–time curves were produced.

Uniaxial tension tests

Tensile specimens were taken along the rolling direction. The parallel gage length was 25 mm long and 6.5 mm wide. The specimens were pulled to fracture at room temperature (~0.65 T_m) at cross-head speeds in the range of 0.5–15 mm min^{-1} to produce initial strain rates of 3.33×10^{-4} s^{-1} to 1.0×10^{-2} s^{-1}, respectively. Load-extension and the corresponding true stress–true strain curves were obtained over the whole gage length, from which the true stress at the peak load was calculated as the flow stress needed for the calculation of stress exponent (n).

Results

Indentation tests

The indentation creep data were measured at room temperature under loads of 20, 30 and 50 N. The results are shown in Fig. 2, where the indentation length is plotted against time. It can be seen from these figures that the indentation length increases with the loading time and the applied load. The three aforementioned methods of Mulhearn and Tabor [31], Juhasz et al. [32] and Sargent and Ashby [28] have been applied to the indentation data of the materials to obtain the steady-state creep exponent. In the Mulhearn–Tabor method, Fig. 3, Vickers hardness number is plotted versus dwell time on a log–log scale for the indentation data. It is observed that there exists a linear relationship between dwell time and hardness for all conditions. Figure 4 plots the rate of diagonal variation against the Vickers hardness number on a double logarithmic scale in accordance with Eq. 3, where $\dot{d}$ was obtained by differentiation of the curves shown in Fig. 2. Figure 4 shows that in both materials similar linear behavior is observed in terms of the slope of the curves. The data plotted according to the Sargent–Ashby analysis are illustrated in Fig. 5 for all materials and testing loads at a constant temperature. The interesting feature of all three methods is that for each material the fitted lines are almost parallel, implying that the stress exponent is independent of the applied load. The stress exponent values obtained for each alloy via each of the abovementioned approaches are represented in Table 1.

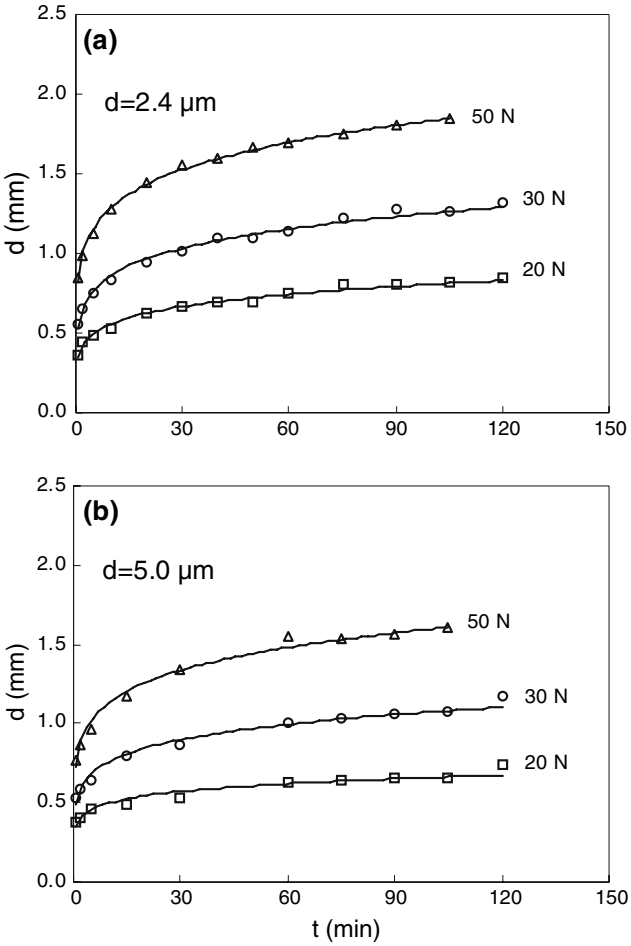

Fig. 2 Indentation creep curves at different loads

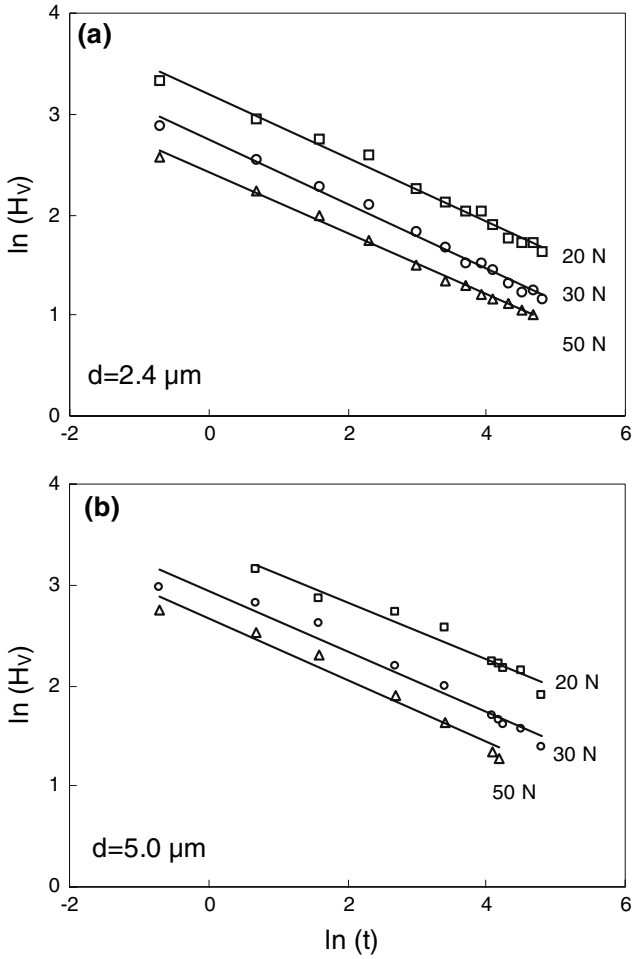

Fig. 3 Data shown in Fig. 2 plotted in accordance with Eq. 2

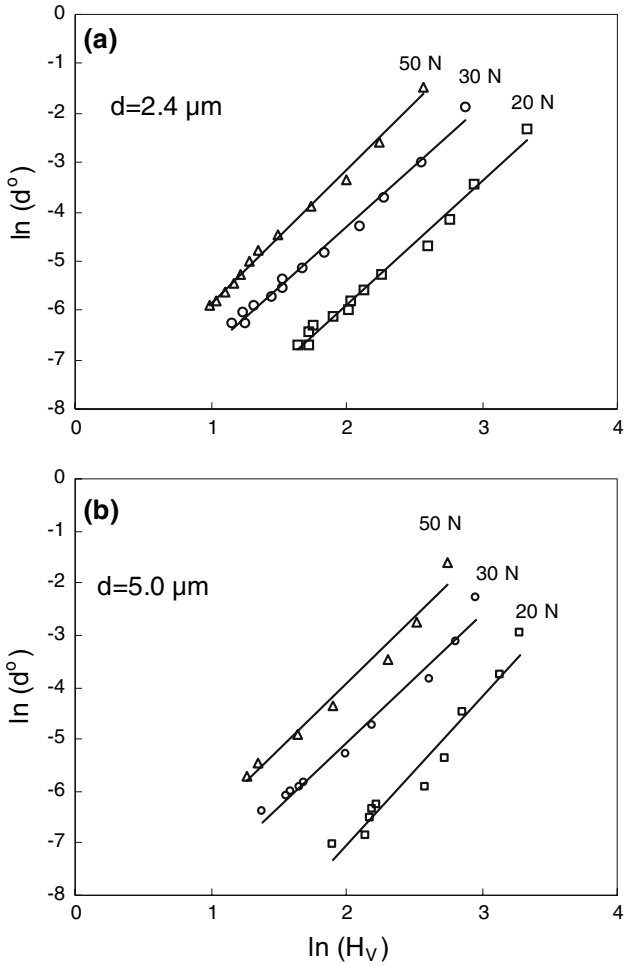

Fig. 4 Data shown in Fig. 2 plotted in accordance with Eq. 3

Conventional creep tests

The creep strain vs. time results obtained from specimens tested under constant load tensile creep are shown in Fig. 6. As shown in this figure, after applying a load to each specimen, the strain increased with time until creep fracture occurred. After differing periods of primary creep, secondary creep behavior characteristics were exhibited, the effect being more pronounced at lower stress levels. From the creep curves, these secondary creep rates were calculated by plotting creep rate versus creep strain and used to obtain n values for both alloys by plotting steady-state creep rate against applied stress and obtaining the n value from the slope of the fitted line. The calculated n values are given in Table 1.

Tension tests

In order to find the stress exponent values from tensile tests, load-extension curves were obtained at different initial strain rates from which, stress–strain curves were determined for both materials as shown in Fig. 7. Different applied strain rates resulted in different material behavior in terms of tensile strength, maximum uniform elongation and elongation to failure. The true stress at the peak load was then determined for each strain rate condition. Figure 8 shows the variation of strain rate against true tensile strength on a double logarithmic scale, a straight line is obtained with the slope of stress exponent n. For comparison, the conventional creep data are superimposed on the tension test data in Fig. 8. The stress exponent values obtained from the tension tests are also given in Table 1.

Discussion

Indentation creep

According to the elastic-plastic analysis of the hardness test [33], when an indenter is pressed into the flat

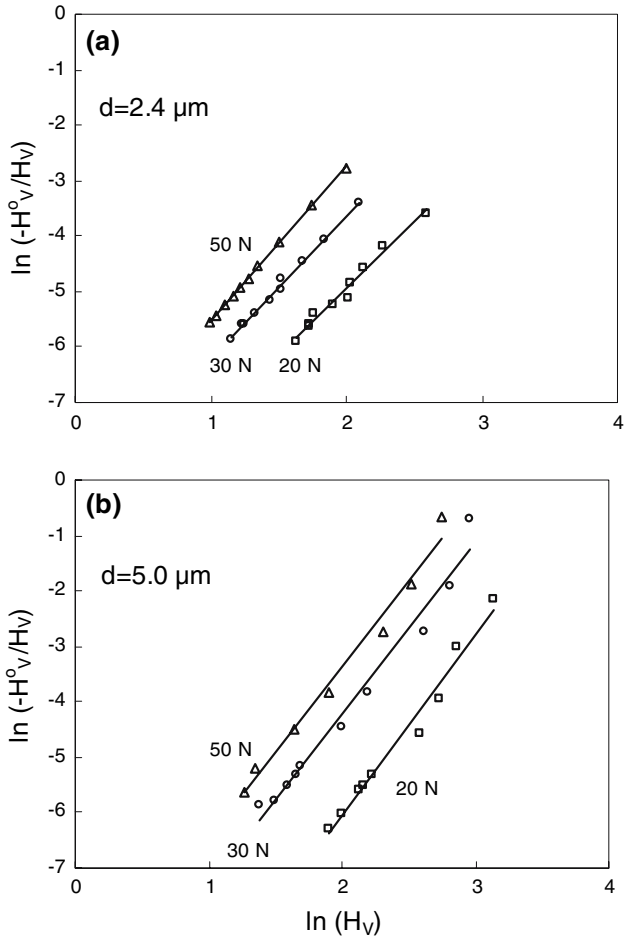

Fig. 5 Data shown in Fig. 2 plotted in accordance with Eq. 7

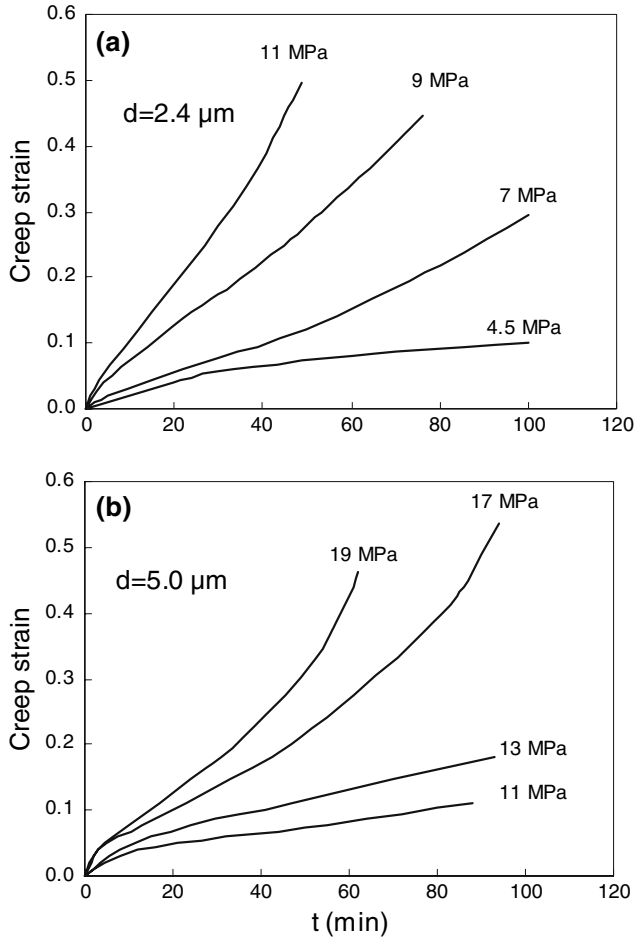

Fig. 6 Conventional creep curves at different stress levels

surface of a solid, the indenter is encased in a non-deforming hemispherical core of material, within which there is assumed to be a hydrostatic pressure. Outside this core, there exists an elastic-plastic hemispherical zone surrounding the hydrostatic zone. The process of indentation is thus linked to the plastic movement of a series of shells concentric with the hemispherical core. It is generally accepted that within the core, the stresses are hydrostatic and here there can be no creep deformation since there are no shear stresses and no chemical potential gradients. Outside the core in the elastic-plastic zone, however, the stress field is deviatoric and this exerts forces on defects present, such as dislocations, vacancies, etc. causing creep. Therefore, with increasing applied load, the deviatoric stress field beneath the indenter increases and the indentation creep process occurs more readily.

Table 1 Stress exponents (n) derived from indentation, creep and tensile tests

Material	Stress exponent (n)					
	Indentation tests				Creep tests	Tensile tests
	Load (N)	Mulhearn-Tabor [29]	Juhasz et al. [30]	Sargent–Asby [26]		
A (d = 2.4 μm)	20	2.55	2.48	2.51	2.6	2.6
	30	2.53	2.45	2.53		
	50	2.60	2.58	2.56		
B (d = 5.0 μm)	20	2.85	2.85	2.90	3.2	3.1
	30	2.74	2.71	2.77		
	50	2.78	2.71	2.79		

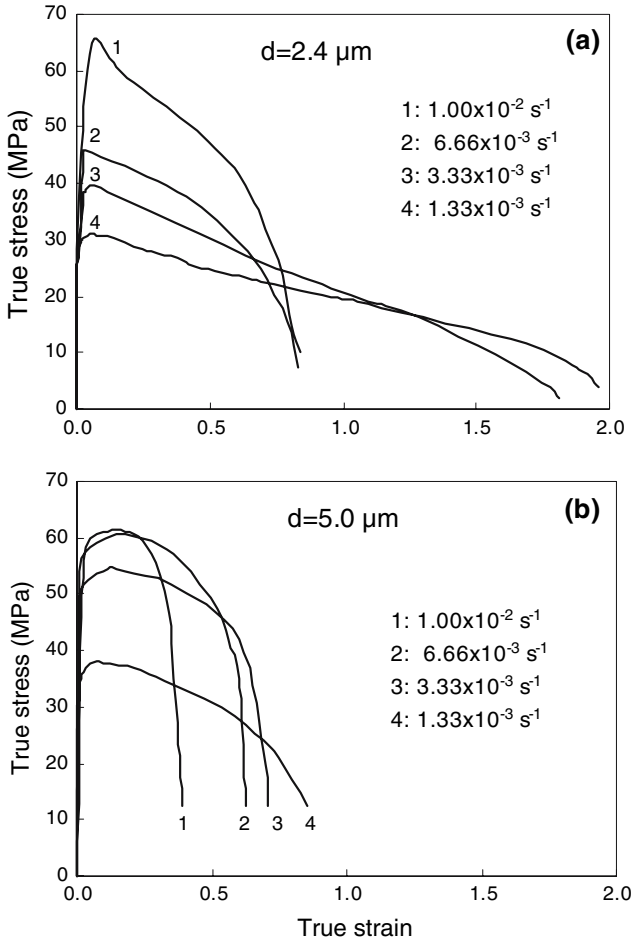

Fig. 7 True stress–true strain curves obtained at different initial strain rates in tension tests

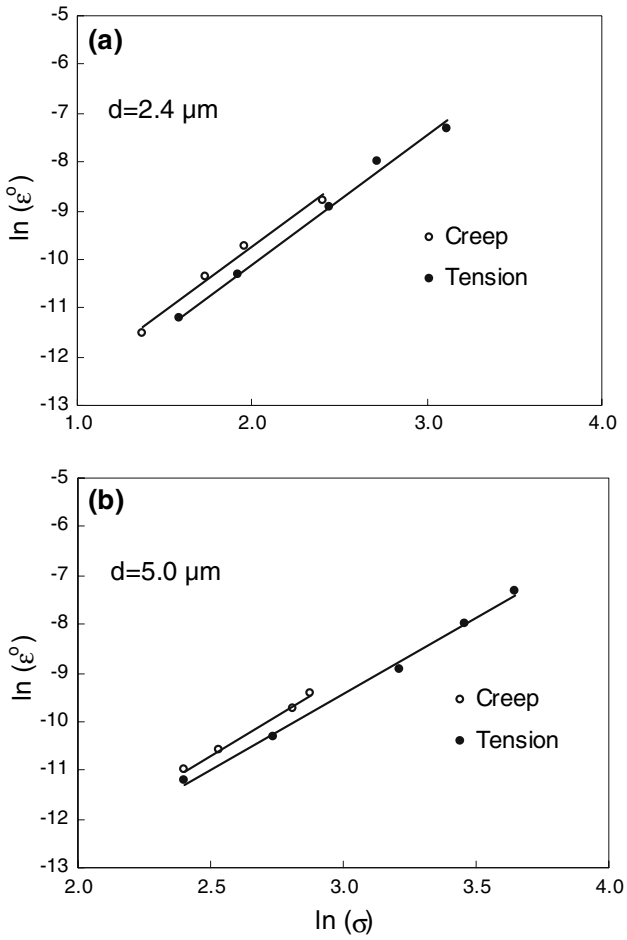

Fig. 8 The variation of strain rate with true tensile stress in tension and creep tests

Typical indentation diagonal-time curves, shown in Fig. 2, consist of two stages similar to an ordinary creep curve. The first stage of the curve records an increase in the concerned variable with time, with the decreasing rate, followed by a steady-state region where indentation sizes increase linearly with time. As the hardness test is actually a compression test, fracture of the specimen does not occur and hence it is obviously not possible to record a third stage of the curve as opposed to what happens in an ordinary creep test. Figure 2 also indicates that different conditions of the material exhibit different indentation creep behaviors. It can be inferred from this figure that the level of indentation curves and their slopes in the steady-state region are higher for condition *A* with a grain size of 2.4 μm while for condition *B* with a grain size of 5 μm there is not much increase in indentation length at lower loads of 20 and 30 N. Thus, indentation creep in the material with a finer grain size happens more readily as compared to the coarser grained material.

The stress exponent values obtained through indentation methods are in the range of 2.45–2.65 and 2.7–2.9 for the materials *A* and *B*, respectively. The stress exponents calculated by different approaches are in good agreement with each other, indicating the similarity of the derivation methods. The experimental results given in Table 1, demonstrate that stress exponent values for both conditions do not depend on the applied load and in all loading conditions, *n* values are almost the same. Another useful finding is that the relation proposed by Mulhearn–Tabor [31] is applicable to hardness tests with Vickers indenter, although Mulhearn's equation is based on a spherical indenter. According to the power law creep, a decrease in stress exponent would result in an increase in creep rate due to a decrease in yield strength [15, 34]. Therefore, material *B* with higher *n* values is more resistant to indentation creep compared to the material *A*. The same result can also be extracted from the indentation curves shown in Fig. 2.

Under the experimental conditions where the power law creep relation is valid, the value of stress exponent can be used to identify the mechanisms controlling the deformation process [35, 36]. In fact, deformation of polycrystalline materials at temperatures above $0.5T_m$ can take place by different deformation mechanisms, associated with different stress exponent values. It is reported that diffusional creep is associated with n values around 1 [30, 37], grain boundary sliding leads to n values close to 2 [34, 38], dislocation climb is responsible for n values in the 4–6 range [19]. Mechanisms associated with dislocation movement such as dislocation creep are attributed to $n > 6$ [18]. Although the stress exponents have been frequently used to identify the mechanisms controlling the deformation process, it should be cautioned that making mere comparisons of the stress exponents, without additional information on activation energies, does not provide sufficient information to draw insightful comparisons on creep mechanisms of materials. At best, creep stress exponents can only help to narrow the field among many theoretical possibilities.

In the present investigation, the observed difference in the indentation behavior of the A and B conditions can be attributed to the grain sizes of these materials. For material A, with a grain size of $d = 2.4$ μm the stress exponent, n, is about 2.6 while for the condition B with $d = 5$ μm, it is about 3.0. This behavior is in agreement with the Gifkins' core-mantle theory suggesting that for a constant width of mantle, an increasingly fine grain size results in a domination of the mantle behavior and thus, the creep exponent begins to decrease [39]. The obtained stress exponents would result in $m = 1/n$ values of 0.39 and 0.33 for the A and B conditions, respectively. It is well accepted that at these relatively high values of SRS index, superplastic deformation mechanisms such as grain boundary sliding become prominent and creep process takes place readily [19, 33–35]. As a support for this argument, one of the samples was optically examined after indentation test. This is shown in Fig. 9, where the grain boundaries surrounding the indent are visible, indicating that during the indentation creep grain boundary sliding has occurred to some extent. Similar behavior has been reported by Juhasz et al. [32], who obtained stress exponent values in the range of 2–2.5, corresponding to strain rate sensitivity (SRS) indices of about 0.45–0.5 for a lead–tin eutectic alloy. This represents a superplastic deformation behavior in which, grain boundary sliding occurs during indentation creep process.

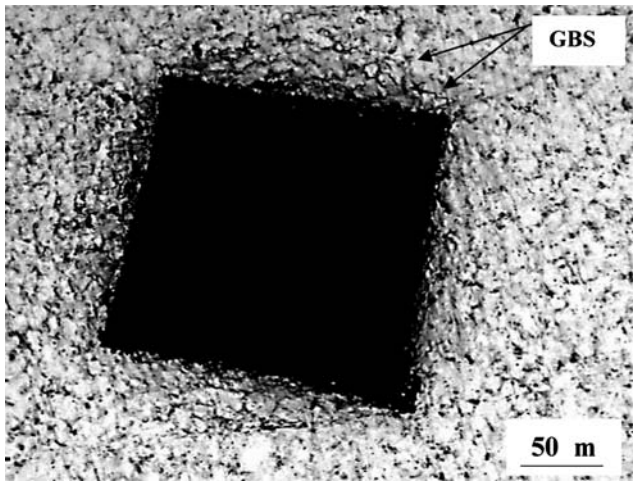

Fig. 9 Optical micrograph of a sample after indentation test

Conventional creep and tension tests

True stress–true strain curves obtained at different strain rates indicated that both materials have reasonably high positive SRS, i.e.; their strength increase by increasing strain rate. Almost in all cases, the maximum strength reached after a relatively small amount of strain, after which, the strength decreased gradually with increasing strain. This effect is more pronounced at low strain rates, where there is no apparent steady state in the curves. A straight forward explanation for this behavior is that the initial stress increase is due to dislocation generation. In other words, the limited range of uniform deformation is associated with the strain necessary for the rearrangement and coarsening of the dislocation structure. At low strain rates, once the maximum strength is reached, the rate of decrease of the dislocation density (annihilation) increases and this leads to a continuously falling stress level.

The stress exponent values obtained from conventional uniaxial creep and tensile tests given in Table 1 are in good agreement with the indentation results. This is ascribed to the equiaxed fine-grained structure of these wrought alloys. In any case, the better agreement that is always found for fine-grained material is due to the number of grains which take part in the deformation process. When a material has a coarse grain size structure, the grain size is of the same order of magnitude as the size of the indentation and it is more difficult to establish an analogy between tensile and creep tests, where a large number of grains take part in the creep process and indentation methods. However, in fine-grained materials, such as the present superplastic alloys, a large number of grains take part in

indentation process and therefore, the results are very similar to those of conventional tensile and creep tests.

As shown in Fig. 6, the shape of creep curves depends upon the applied stress. Although the curves for different conditions are not plotted up to the occurrence of fracture, typical creep stages are observed for some cases at lower values of stress. With increasing the applied stress, however, the steady-state region becomes shorter and creep fracture happens more readily. For a given stress level (e.g. 11 MPa), the creep curves of material *A* are much steeper than those of the *B* material, implying a higher steady-state creep rate in the former material.

Conclusions

(1) It is experimentally demonstrated that an indentation creep process occurs in the Sn–Pb–Sb peritectic alloy at room temperature. The data analyses have also shown that the simple theory, based on steady-state power-law creep equation, has the capacity to describe the indentation creep data satisfactorily.

(2) The stress exponents calculated from different methods of analysis are independent of the loading conditions and are in complete agreement with each other. These exponents have been determined by indentation methods to evaluate their applicability as compared with tensile and creep tests. The results of indentation methods are in good agreement with conventional creep and uniaxial tensile tests.

(3) The creep process can be characterized by the stress exponents. The average stress exponent values obtained from different methods were found to be about 2.6 and 3.0 for the finer and coarser-grained conditions, respectively. These stress exponents correspond, respectively, to average SRS indices of 0.39 and 0.33, suggesting that the room-temperature creep of the Sn–Pb–Sb peritectic alloy is a superplastic process. These relatively high *m* values imply that grain boundary sliding is most probably the dominant creep mechanism in this peritectic alloy at room temperature.

(4) The indentation creep test is thus demonstrated to be effective in evaluating creep behavior of materials using small specimens. It is further demonstrated that the indentation creep test provides a convenient method to measure SRS and thereby to assess the ability of a material to undergo superplastic deformation.

Acknowledgements The authors thank the Research Council of Tehran University for providing financial support of this work under Grant No. 615/4/798.

References

1. Thwaites CJ (1986) Brazing Solder 11:22
2. Hilger JP (1995) J Power Source 53:45
3. Tomlinson WJ, Bryan NJ (1986) J Mater Sci 21:103
4. Fujiwara M, Otsuka M (2001) Mater Sci Eng A319–321:929
5. Juhasz A, Tasnadi P, Szaszvari P, Kovacs I (1986) J Mater Sci 21:3287
6. Yang F, Li JCM (1995) Mater Sci Eng A201:40
7. Manko HH (1992) Solders and Soldering, 3rd edn. McGraw-Hill, New York
8. Mathew MD, Yang H, Movva S, Murty KL (2005) Metall Mater Trans 36A:99
9. Roumina R, Raeisinia B, Mahmudi R (2003) J Mater Sci Lett 22:1435
10. Kutty TRG, Ganguly C, Sastry DH (1996) Scripta Mater 34:1833
11. Roumina R, Raeisinia B, Mahmudi R (2004) Scripta Mater 51:497
12. Cseh G, Chinh NQ, Juhasz A (1998) J Mater Sci Lett 17:1207
13. Hooper RM, Brookes CA (1984) J Mater Sci 19:4057
14. Viswanathan UK, Kutty TRG, Keswani R, Ganguly C (1996) J Mater Sci 31:2705
15. Cseh G, Chinh QN, Tasnadi P, Juhasz A (1997) J Mater Sci 32:5107
16. Giacometti E, Baluc N, Bonneville J, Rabier J (1999) Scripta Mater 41:989
17. Cseh G, Bar J, Gudladt HJ, Lendvai J, Juhasz A (1999) Mater Sci Eng A272:145
18. De La Torre A, Adeva P, Aballe M (1991) J Mater Sci 26:4351
19. Sharma G, Ramanujan RV, Kutty TRG, Tiwari GP (2000) Mater Sci Eng A278:106
20. Yu HY, Imam MA, Rath RB (1986) Mater Sci Eng A79:125
21. Kumar N, Raman KS, Sastry DH, Little EA (1990) J Mater Sci 25:753
22. Chinh NQ, Juhasz A, Tasnadi P, Kovacs I (1990) J Mater Sci 25:4767
23. Hyde TH, Yehia KA, Becker AA (1995) Mater High Temp 13:133
24. Dorner D, Roller K, Skrotzki B, Stockhert B, Eggler G (2003) Mater Sci Eng A357:346
25. Fang TT, Kola RR, Murty KL (1986) Metall Trans 17A:1447
26. Rani SD, Murthy GS (2004) Mater Sci Technol 20:403
27. Dutta I, Park C, Choi S (2004) Mater Sci Eng A379:401
28. Sargent PM, Ashby MF (1992) Mater Sci Technol 8:594
29. Lucas BN, Oliver WC (1999) Metall Mater Trans 30A:601
30. Langdon TG (2000) Mater Sci Eng A283:266
31. Mulhearn TO, Tabor D (1960) J Inst Metals 89:7
32. Juhasz A, Tasnadi P, Kovacs I (1986) J Mater Sci Lett 5:35
33. Li WB, Henshal JL, Hooper RM, Easterling KE (1991) Acta Metall Mater 39:3099
34. Walser B, Sherby OD (1982) Scripta Metall 16:213
35. Sherby OD, Wadsworth J (1989) Prog Mater Sci 33:169
36. Frost HJ, Ashby MF (1982) Deformation mechanism maps. Pergamon, Oxford
37. Ashby MF, Verrall RA (1973) Acta Metall 21:149
38. Mukherjee AK, Bird JE, Dorn JE (1969) ASM Trans 62:155
39. Gifkins RC (1976) Metall Trans 7A:225